

Crossover between ordinary and normal transitions in the presence of a bulk field

A. Maciołek,¹ A. Drzewiński,² and A. Ciach¹

¹*Institute of Physical Chemistry, Polish Academy of Sciences, Department III, Kasprzaka 44/52, PL-01-224 Warsaw, Poland*

²*Institute of Low Temperature and Structure Research, Polish Academy of Sciences, P.O. Box 1410, Wrocław 2, Poland*

(Received 26 January 2001; published 25 July 2001)

We investigate two-dimensional Ising films at the critical temperature T_c and nonzero bulk magnetic field h using the density-matrix renormalization-group method. The crossover between ordinary ($h_1=0$) and normal ($h_1=\infty$) transitions corresponding to finite values of the surface fields $h_1=h_2$, is studied. The structure and the solvation force f_{solv} as a function of h , crucially depend on the value of h_1 . Scaling functions for f_{solv} and the longitudinal correlation length are given and discussed.

DOI: 10.1103/PhysRevE.64.026123

PACS number(s): 64.60.Fr, 05.50.+q, 68.35.Rh

I. INTRODUCTION

The Ising film of a finite width L with fields h_1, h_2 acting on two surfaces, serves as an idealized representation of a fluid in a slitlike pore or between two large colloidal particles; the local surface fields model the substrate-fluid interactions, which give rise to adsorption phenomena. Studies of these model systems provide theoretical input for understanding adsorption experiments in porous materials or finely divided colloidal graphite and for interpreting surface force apparatus or atomic force microscope [1] measurements of the liquid mediated forces (solvation forces) between two substrates separated by microscopic distances. Properties of the solvation force f_{solv} are also relevant for the behavior of colloids, in particular, for the form of the equation of state, since f_{solv} contributes to effective interactions between large colloidal particles immersed in a fluid. The strength, range, and the structure of the solvation force depend on the thermodynamic state of a system (T, μ) but also on the adsorption properties of confining substrates, i.e., on the value of h_1 and h_2 in the model system.

In this paper we focus on the case of identical walls $h_1 = h_2 > 0$ and investigate the behavior of near-critical Ising films for different h_1 . Near the bulk criticality of a fluid, the dependence of various physical quantities on h_1 is especially pronounced since the bulk correlation length becomes macroscopically large and the effect of walls extends into the whole system. The leading critical behavior of a system in the presence of a surface, is classified into four different surface universality classes depending on whether the ordering at the surface is enhanced or de-enhanced compared to the bulk [2,3]. The most relevant for fluids in contact with adsorbing walls is the normal transition when the external field h_1 breaks the symmetry at the surface, inducing ordering in the surface layer. The corresponding fixed point of the renormalization-group transformation is related to $h_1 = \infty$ and to the surface enhancement of the interaction $c = \infty$ [3]. In the real confined fluids, the distance between the confining substrates is often too small to observe the leading critical behavior and the properties of a system at the finite h_1 , i.e., in the crossover between the normal and the ordinary $h_1 = 0$, $c = \infty$ fixed points, become relevant. The above crossover was studied in the two-dimensional ($d=2$) Ising films

of the finite width L at the bulk critical point $T=T_c$, and the bulk magnetic field $h=0$ [4]. A peculiar behavior of the solvation force was found for weakly adsorbing walls: the scaling function for $|f_{solv}(h_1)|$ exhibits a deep minimum near $L=h_1^{-\nu/\Delta}$ associated with unusual order parameter (OP) profiles that increase from the walls; ν and Δ_1 are the critical indices [3].

Whereas the mechanism leading to the OP profiles of a shape so different from ones corresponding to fixed points $h_1=0$ and $h_1=\infty$, can be explained heuristically on the basis of the behavior of correlations in the near-surface region [5], it is not immediately obvious why at the bulk critical point f_{solv} should be less attractive for weak h_1 .

In order to better understand the structure of the solvation force in the crossover region, we ask the question how does the density of the confined fluid affect f_{solv} and other quantities for finite h_1 . The case of the vanishing h studied in Ref. [4] corresponds to a fluid at the critical density. Here we are interested in a situation more relevant for experiments, i.e., when the density slightly deviates from its critical value. In the Ising system this situation corresponds to $|h| < 1$. Recent studies show that in the case of strongly adsorbing walls ($h_1 = \infty$) the presence of even a very weak negative bulk field may lead to pronounced effects near T_c , such as a dramatic change of the adsorption (critical depletion) [6,7] or a significant increase of $|f_{solv}|$ [8]. The latter effect is related to the phase behavior of the confined fluid below T_c . Capillary condensation, i.e., the shift of the bulk first-order transition, which occurs below T_c , influences the behavior of f_{solv} at $T=T_c$, leading to the very attractive force away from $h=0$ [9]. It then follows that more information about the structure of the solvation force in the crossover region can be inferred from the study of its behavior as a function of h for different values of h_1 between 0 and ∞ . Thanks to the recently developed density-matrix renormalization-group (DMRG) method, such systematic studies at $T=T_c$, are possible in $d=2$. DMRG is an approximate technique based on the transfer-matrix approach [10]. The accuracy of this method at $T=T_c$, $h=0$ and different surface fields h_1 between 0 and 10, was tested in Ref. [4] by comparison with the results obtained using the exact diagonalization of the transfer matrix. The agreement of calculated quantities such as f_{solv} or magnetization profiles was remarkable. The same

method was then successfully applied to study the effect of the bulk field at fixed points $T=T_c$, $h_1=0$ (ordinary transition), and $h_1=\infty$ (normal transition) [8]. The present paper completes the study of critical $d=2$ Ising films with arbitrary bulk and surface fields. The paper is organized as follows. Section II defines the model, Sec. III briefly describes the technique and presents our results. Section IV summarizes our conclusions.

II. THE MODEL

We consider the $d=2$ Ising film defined on the square lattice $L \times M$, $M \rightarrow \infty$. The lattice consists of L rows at spacing $a \equiv 1$, so that the width of the film is $La=L$. At each site, labeled i, j, \dots , there is an Ising spin variable taking the value $\sigma_i = \pm 1$. We assume nearest-neighbor interactions of strength J and a Hamiltonian of the form

$$\mathcal{H} = - \left[J \sum_{\langle i,j \rangle} \sigma_i \sigma_j - H \sum_i \sigma_i - H_1 \sum_i \sigma_i - H_2 \sum_i \sigma_i \right], \quad (1)$$

where the first sum runs over all nearest-neighbor pairs of sites, while the last two sums run, respectively, over the first and the L th row. $H=hJ$ is the bulk magnetic field, $H_1=h_1J$ and $H_2=h_2J$ are surface fields corresponding to direct, short-range (“contact”) interactions between the walls and the spins in the film. We assume that $h_1=h_2>0$.

Scaling fields describing the deviation from the bulk criticality are $\tau \equiv (T-T_c)/T_c$ and h . The presence of a wall introduces an additional field: the surface field h_1 . The length scales related to the above scaling fields are $l_\tau = \mathcal{A}_\tau \tau^{-\nu}$, $l_h = \mathcal{A}_h h^{-\nu/\Delta}$, and $l_1 = \mathcal{A}_{h_1} h_1^{-\nu/\Delta_1}$, where the critical indices $\Delta = 15/8$, $\nu = 1$, and $\Delta_1 = 1/2$ in the $d=2$ Ising model. At vanishing bulk magnetic field the bulk correlation length ξ_b reduces to l_τ , whereas at the critical temperature, ξ_b reduces to l_h . The remaining length scale l_1 describes the distance from the wall up to which the system responds linearly to a weak surface field h_1 near bulk criticality. Although at the critical point the system no longer responds linearly to the external field, the boundary layer remains paramagnetic for $h_1 \rightarrow 0$. This is due to the missing neighbors, which cause the effective interaction per spin at the boundary layer weaker than in the bulk. The paramagnetic phase at the boundary layer does not abruptly change into the critical system in the subsequent layers, but rather extends smoothly to the distance $\sim l_1$ from the wall [4].

III. DENSITY-MATRIX RENORMALIZATION-GROUP RESULTS

The DMRG method, originally introduced to study quantum spin chains [10], provides an efficient algorithm to construct the effective transfer matrix also for large $d=2$ classical systems [11]. Applying this technique one deals with spin variables and effective blocks describing collections of spins [12]. The linear dimension of the total effective transfer matrix is $4m^2$. In the present case we found that the value of

states kept in a block $m=40$ is sufficient to guarantee a very high accuracy of results.

As in Ref. [8] we have used the finite-system version of the DMRG algorithm designed to perform accurate studies for finite-size systems [10,13]. In order to improve results, one performs here more DMRG iterations keeping the system size fixed, whereas the number of spins included in effective blocks is changed. The procedure is time consuming, but fortunately, in our case, only one cycle of iterations (called a sweep) is sufficient to get practically saturated results.

Calculations were performed for films of width L equal to 100, 150, and 200 at T_c . In the transfer-matrix approach the leading eigenvalue λ_L of the transfer matrix T_L ,

$$T_L |v_L\rangle = \lambda_L |v_L\rangle, \quad (2)$$

gives the free energy per spin of an Ising film as

$$\beta f(L) = -\frac{1}{L} \ln \lambda_L. \quad (3)$$

In the DMRG method, the leading eigenvalue of the *effective* transfer matrix is calculated numerically. At a fixed surface field h_1 , ranging from 10^{-7} to 10, we calculate various physical quantities for the bulk magnetic field $|h| < 1$.

A. Solvation force

In order to find the solvation force at $T=T_c$, we first calculate the excess free energy per unit area $f^{ex}(L) \equiv (f(L) - f_b)L$, where f_b is the bulk free energy per spin. f_b is known exactly for the 2D Ising model at $T=T_c$ and zero bulk field [14], and its numerical value is approximately equal to $f_b \cong -2.1096511$. For a nonzero bulk field we have to evaluate it numerically. At this point it is worth making a digression about the accuracy of the results. For the bulk system, when we reach the critical point along the isotherm $T=T_c$, the correlation length grows as $\xi = \mathcal{A}_h h^{-\nu/\Delta}$ and diverges at the critical point. In order to set the bulk free energy per spin at a certain value of h from the numerical calculations, we find the values of the free energy for the finite systems (strips) with larger and larger widths L and extrapolate them for $L \rightarrow \infty$ using the Bulirsch and Stoer method. An extrapolation guarantees a high accuracy of the bulk free energy, if the ratio between the width of the largest strip L_{max} and the correlation length is much greater than 1; the smaller L_{max}/ξ is the less accurate are the extrapolated values. Of course, generally the lowest accuracy of the bulk free energy gives the worst accuracy of the solvation force (see below). As a compromise between the accuracy and time of calculations, $L_{max}=300$ was chosen in our case. To get better results for small h , where $\xi \gg L$ and the extrapolation is poor, we decided to use the approximate formula $f_b(h) = f_b(h=0) - 0.9399/(1/\delta+1)|h|^{1/\delta+1}$, based on the following dependence $m_b(h) \sim \text{sgn}(h)|h|^{1/\delta}$ at $T=T_c$ (for more details see Ref. [8]), where $\delta=15$ in the $d=2$ Ising model. On the basis of the analysis of the results, we have chosen $|h|=0.000055$ as the border value of the bulk field, where which the approximate formula is used below,

whereas above, the extrapolation of the DMRG results is done. In spite of some deviations, both curves coincide satisfactorily.

The solvation force for our system is defined as

$$f_{solv} = -(\partial f^{ex}/\partial L)_{h,T}. \quad (4)$$

In our calculations we approximate the derivative in Eq. (4) by a finite difference

$$f_{solv} = -(1/2)[f^{ex}(L_0+2) - f^{ex}(L_0)]. \quad (5)$$

From the general theory of critical finite-size scaling [15] it follows that the solvation force for identical surface fields should take the following scaling form

$$f_{solv}/k_B T_c = L^{-d} \mathcal{F}(L/l_\tau, L/l_h, L/l_1), \quad (6)$$

where \mathcal{F} is a universal scaling function. At fixed points $\tau = 0$, $h = 0$, and $h_1 = 0$, or $h_1 = \infty$ the leading-order decay of the solvation force for $L \rightarrow \infty$ is algebraic since the scaling function reduces to $\mathcal{F}(0,0,0) = \mathcal{A}_0 k_B T_c$ or $\mathcal{F}(0,0,\infty) = \mathcal{A}_\infty k_B T_c$. \mathcal{A}_0 and \mathcal{A}_∞ are the universal, so-called, Casimir amplitudes. For the $d=2$ Ising model, $\mathcal{A}_\infty = \mathcal{A}_0 = -\pi/48$.

In order to study the crossover region at $\tau=0$, we ignore nonuniversal metric factors and calculate $L^{-d} f_{solv}/k_B T_c$ as a function of

$$y \equiv \text{sgn}(h)L|h|^{v/\Delta} \quad (7)$$

at several fixed values of x :

$$x \equiv L|h_1|^{v/\Delta_1}. \quad (8)$$

The obtained scaling function $F(0,y,x)$ is presented in Fig. 1, for $x=0, 0.02, 0.25, 1, 5$, and $20\,000$. The functions $F(0,y,0)$ and $F(0,y,20\,000)$, corresponding to ordinary and normal fixed points, respectively, were obtained in Ref. [8]. The shape of these functions differ very much from each other: $F(0,y,0)$ has two shallow symmetric minima—one located at some $h_{min} > 0$ and the second at $-h_{min}$, whereas $F(0,y,20\,000)$ has a single deep minimum. At the minimum, the absolute value of $F(0,y,0)/k_B T_c$ is approximately 3.8 times the Casimir amplitude \mathcal{A}_0 , while the absolute value of $F(0,y,20\,000)/k_B T_c$ is nearly 100 times \mathcal{A}_∞ . These distinct properties of the solvation force at $T=T_c$ reflect different phase behavior below T_c . Although for bulk $d=2$ systems, there can be no true phase coexistence for finite L , there is still a line of sharp (very weakly rounded) first-order transitions in the Ising film ending in the pseudocritical point [16,17].

In films with free boundaries, the Ising symmetry requires two-phase coexistence to be at $h=0$. Therefore, the sign of the applied bulk field is not relevant for the behavior of the system and two symmetric minima of the scaling function $F(0,y,0)$ occur when a dominant length in the system at $T=T_c$, l_h becomes comparable with L .

In films with surface fields $h_1=h_2>0$, the symmetry is broken and the entire phase boundary in the (T,h) plane [capillary condensation line $h_{co}(T)$] is displaced into the half-plane $h<0$ [9,16,18]. Capillary condensation ends at the

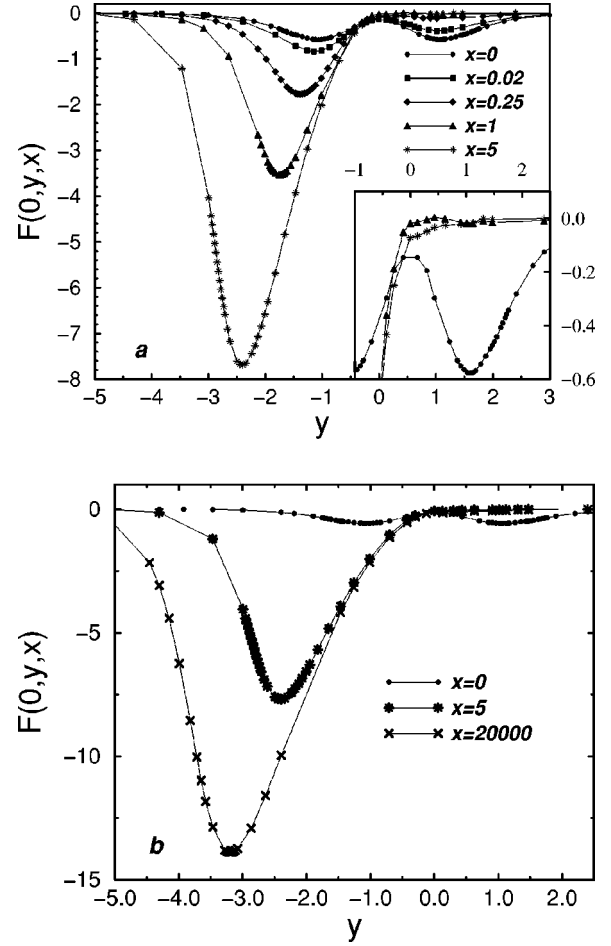


FIG. 1. Scaling functions of the solvation force $F(0,y,x)$ calculated in $d=2$ Ising films of several widths $L=100, 150$, and 200 at $T=T_c$ and fixed values of surface fields $h_1=h_L$ (fixed x). The inset shows the nontrivial behavior of the scaling function in the neighborhood of $y=0$. Scaling functions and scaling variables are dimensionless.

(capillary) critical point (h_{cL}, T_{cL}) , where $T_{cL}(h_1)$ lies below T_c , nevertheless it strongly influences the behavior of the solvation force at T_c , a discontinuous jump of f_{solv} from almost zero to some large negative value, on crossing the coexistence line $h_{co}(T)$, transforms at $T=T_c$ into a single deep minimum located at some $h_{min} < 0$ [9,19].

Other curves in Fig. 1 show how the asymmetric behavior of the scaling function $F(0,y,x)$ sets in when h_1 increases from zero. For weak h_1 , there are still two minima. As the surface field becomes stronger, the minimum located at the positive value of h becomes more shallow and shifts towards $h=0$. At the same time the minimum located at the negative value of h becomes deeper and shifts away from $h=0$. The shape of the scaling function changes in such a way that the absolute value of $F(0,y,x)$ at $h=0$ decreases with the growth of x until $x \approx 1$, i.e., until the minimum at $y>0$ disappears. A further increase of x leads to the increase of $F(0,0,x)$. The maximum of $F(0,0,x)$ occurs for $x \approx 1$, i.e., for $L \sim l_1$ [see Eq. (8)].

For stronger surface fields, i.e., $x>1$, $F(0,y,x) \approx 0$ for $y > 0$ at fixed x and decreases rapidly to a single deep mini-

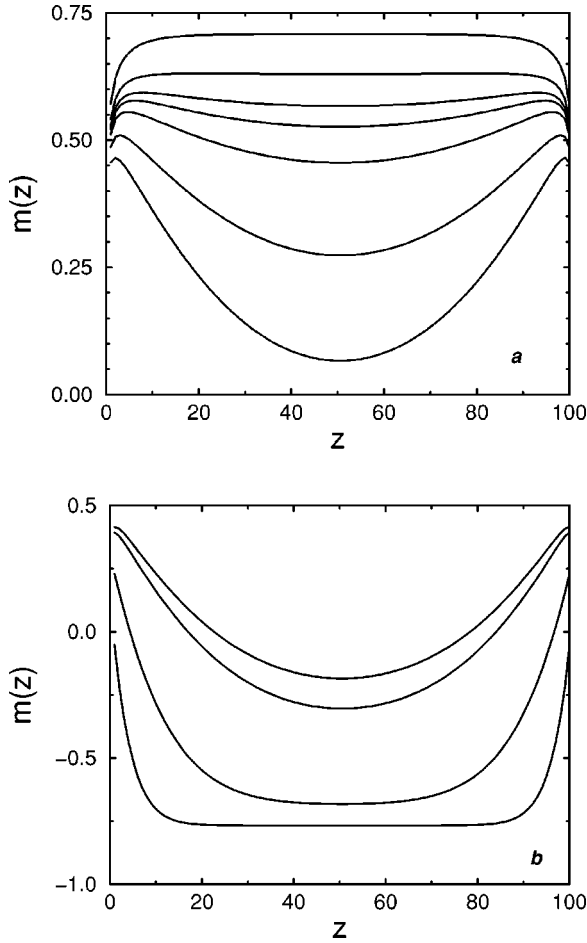


FIG. 2. Magnetization profiles calculated in the $d=2$ Ising film of the width $L=100$ at $T=T_c$ and fixed values of surface fields $h_1=h_L$ such that $x=Lh_1^{v/\Delta_1}=5$. Different curves correspond to different values of the bulk magnetic field: from the top profile to the bottom one: (a) $h=0.0055, 0.0009, 0.0, -0.0003, -0.00055, -0.00088,$ and -0.0013 ; (b) $h=-0.00108, -0.0014, -0.0036,$ and -0.018 . z is in units of the lattice constant, magnetization is dimensionless, h is in units of coupling constant J .

imum at the negative value of y . For small negative values of y , this rapid decrease is linear in h indicating residual condensation [9].

B. Magnetization profiles and the adsorption

As already mentioned in the Introduction, the shape of the magnetization profiles at $\tau=0$, $h=0$ and weak surface fields differs very much from the shape assumed at the fixed point $y=\infty$. The OP profile, corresponding to the normal transition, decreases monotonically towards the center of the film, whereas for weak h_1 , the maximum order is shifted away from the wall to the distance $\sim l_1$. For surface fields such that $1 < l_1 < L$, magnetization profiles at $\tau=0$, $h=0$ have two symmetric maxima. They merge into one, broad maximum located at the middle of the film for $l_1 \sim L$. For $l_1 > L$ the profiles are nearly flat with the magnetization much lower near the walls than in the central part of a system.

In Fig. 2 we show the evolution of the most nontrivial

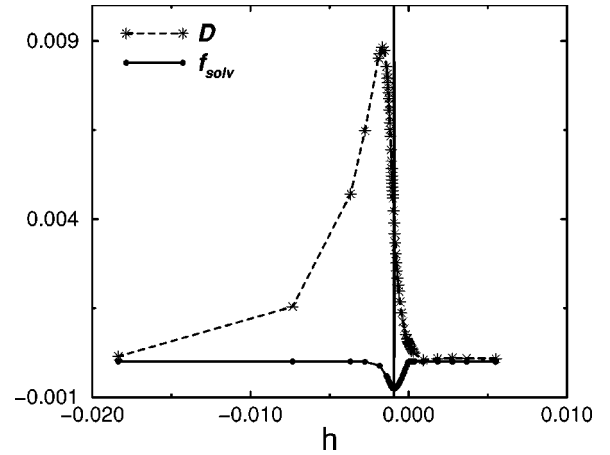


FIG. 3. Parameter D (dimensionless) describing nonuniformity of the magnetization profiles plotted together with the solvation force f_{solv} (in units of J) as functions of the bulk magnetic field (in units of J). Both quantities were calculated for the $d=2$ Ising film of the width $L=100$ at $T=T_c$ and the fixed value of surface fields $h_1=h_L$ such that $x=Lh_1^{v/\Delta_1}=5$.

types of profiles (with two maxima) as a function of the magnetic field. Profiles are calculated for $L=100$ at fixed $\tau=0$ and $x=5$. It is seen that for weak positive h as well as for sufficiently negative h , the profiles are nearly flat except near the walls. They become distinctly nonuniform for h from the neighborhood of the minimum of the solvation force. To make the relation between the minimum of $f_{solv}(h)$ and the nonuniformity of corresponding profiles more quantitative, we define the nonuniformity parameter as

$$D \equiv \frac{1}{L-2l_1} \int_{l_1}^{L-l_1} dz \left| \frac{dm}{dz} \right|. \quad (9)$$

The discrete version of D is given by

$$D \equiv \frac{1}{L-2l_1} \sum_{l_1}^{L-l_1} |m(z) - m(z-1)|, \quad (10)$$

where $m(z)$ is the average magnetization $\langle \sigma_i \rangle$ at the perpendicular distance $z=ia$, $i=1, \dots, L$, from the first wall. The above definition neglects the direct effect of the surface field on the profile in the linear-response layers near surfaces. Thus, D describes the nonuniformity of the central, core part of the slit, which is not responding linearly to the weak surface field h_1 . The parameter D is zero for profiles that are flat in the center of the film and takes a large value for the ones that are highly nonuniform. We calculated D for $m(z)$ presented in Fig. 2 and other profiles corresponding to $x=5$ at different values of h taking the amplitude $\mathcal{A}_{h_1} \approx 0.9091$ in the $d=2$ Ising model [20]. D as a function of the bulk field for $x=5$, is shown in Fig. 3 together with $f_{solv}(h)$. For h near the minimum of the solvation force h_{min} , the function $D(h)$ exhibits a rapid increase and we find that the inflection point of $D(h)$ is located near h_{min} .

The solvation force is closely related to the adsorption Γ_t , which for the Ising film, is defined as follows:

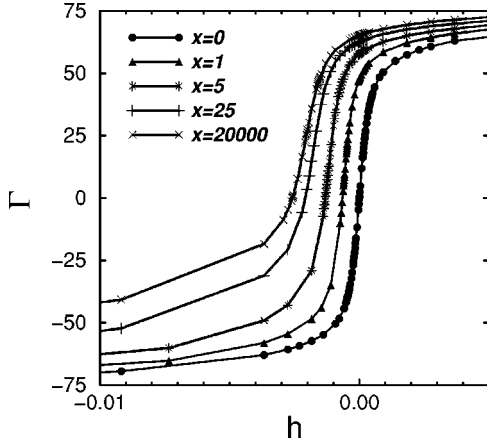


FIG. 4. Adsorption Γ as a function of the bulk magnetic field calculated for the $d=2$ Ising film of the width $L=100$ at $T=T_c$ and several fixed values of surface fields $h_1=h_L$ such that $x=Lh_1^{\nu/\Delta_1}=5$. Γ is dimensionless, h is in units of J .

$$\Gamma_t \equiv \sum_1^L [m(z) - m_b], \quad (11)$$

where m_b is the bulk magnetization at T, h . Thermodynamics implies that at a fixed value of the surface field [19]

$$\left(\frac{\partial f_{\text{sol}v}}{\partial h} \right)_{T,L} = \left(\frac{\partial \Gamma_t}{\partial L} \right)_{T,h}. \quad (12)$$

Therefore, the extremum of the solvation force as a function of the bulk field at fixed T, L is associated with the extremum of the adsorption as a function of the width of a film L at fixed T, h . Our results agree reasonably well with the above predictions.

In Fig. 4 we plot the adsorption $\Gamma \equiv \Gamma_t + Lm_b$ as a function of h for different surface fields. For $x=0$, $\Gamma(h)$ is an odd (antisymmetric) function. As h_1 increases the adsorption grows and its zero moves towards $h < 0$.

C. Longitudinal correlation length

It is instructive to see how the crossover from nonadsorbing to strongly adsorbing walls influences the behavior of the longitudinal spin-spin correlation length ξ_{\parallel} of a finite system. If we take the transfer matrix in the infinite dimension then

$$\xi_{\parallel}^{-1}(\tau, h; L, h_1) = -\ln[\Lambda_1 / \Lambda_0]. \quad (13)$$

Here Λ_0 and Λ_1 are the largest and the second largest eigenvalues of the transfer matrix. Near bulk criticality, ξ_{\parallel}^{-1} obeys scaling (ignoring metric factors):

$$L\xi_{\parallel}^{-1}(\tau, h; L, h_1) \approx K(L^{1/\nu}\tau, y, x) \quad (14)$$

with the appropriate universal scaling function $K(L^{1/\nu}\tau, y, x)$.

In Fig. 5 we present the scaling function $K(0, y, x)$ calculated for the same values of x as the scaling function of the solvation force shown in Fig. 1. Functions $K(0, y, 0)$ and $K(0, y, 20000)$, corresponding to ordinary and normal fixed

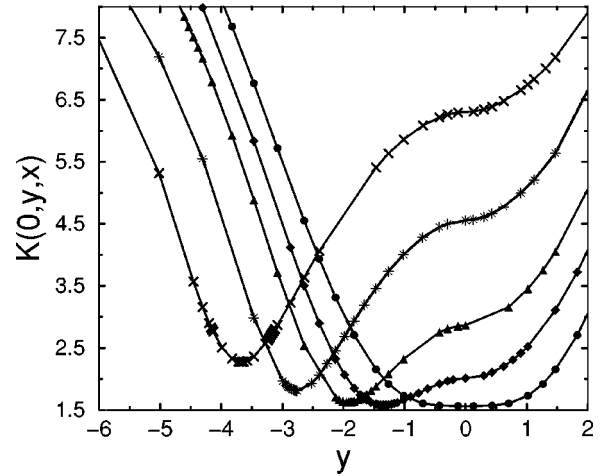


FIG. 5. Scaling functions $K(0, y, x)$ of the inverse of the longitudinal spin-spin correlation length of finite system ξ_{\parallel} , calculated for the same systems as in Fig. 1. Symbols corresponding to different x are the same as in these figures. Scaling function and scaling variables are dimensionless.

points, respectively, were obtained in Ref. [8]. $K(0, y, 0)$ is an even (symmetric) function with the largest value of the correlation length located at $y=0$ (critical point). From the plot it is seen how the asymmetry of the scaling function builds in when h_1 becomes nonzero. As x increases, the minimum of $K(0, y, x)$ (maximum ξ_{\parallel}) for fixed x , shifts to negative values of y and the value of the scaling function increases for all values of y including the minimum (ξ_{\parallel} decreases). This means that in the presence of surface fields the longitudinal correlation length becomes smaller than in the case of free boundaries, i.e., adsorbing walls suppress fluctuations. The minima of $K(0, y, x)$ at fixed x lies close to the maxima of the nonuniformity parameter $D(h)$, thus, they are associated with highly inhomogeneous profiles. $\xi_{\parallel}(h)$ for h around its maximum is much larger than the corresponding bulk “magnetic” correlation length l_h due to a presence of broad interfaces between thin layers of a liquidlike phase near the walls and a gaslike phase in the middle of the film. Around $y=0$, all curves are nearly constant, which reflects the finite-size effects $\xi_{\parallel} \sim L$. L/ξ_{\parallel} becomes a linear function of y for sufficiently large $|y|$ with the same slope for all studied x .

IV. DISCUSSION

The present paper completes the study of $d=2$ Ising films at $T=T_c$ in the whole range of the bulk h and surface h_1 external fields. With the help of the DMRG method, we have obtained very accurate results. The structure, as described by magnetization profiles, the adsorption and the longitudinal correlation length, as well as mechanical properties, i.e., the solvation force, and all the corresponding scaling functions, are given. The scaling functions we present are the only available universal quantities for the whole crossover region $0 < h_1 < \infty$ on the critical isotherm $h \neq 0$ for the Ising universality class in $d=2$.

The behavior of the structure and the solvation force in the crossover region is very rich, which is of relevance for

experiments. Competition between the surface and the bulk fields, favoring the positive or the negative magnetization, respectively, leads to highly nonuniform OP profiles associated with the largest longitudinal correlation length and the most attractive solvation force. The peculiar behavior of f_{solv} at bulk criticality, i.e., a deep minimum of the scaling function $F(0,0,x)$ near $L \sim l_1$, results from its global properties. The surface field corresponding to $l_1 \approx L$ is a border value for qualitatively different shapes of $f_{solv}(h)$, with two minima below and the one minimum above this value.

For temperatures slightly above and below the critical temperature, we expect similar behavior. In fact, magnetization profiles with two maxima near the walls, characteristic for weak surface fields, were found in the Monte Carlo simulations of the $d=2$ Ising film of the width $L=24$, $h_1=0.25$, and $T/T_c=0.95$ [21]. This paper was devoted to the study of the shift of phase boundary due to boundary fields in Ising systems with identical walls and the authors did not connect the somewhat surprising shapes of the obtained profiles with the (weak) value of the surface field.

What is the relation between our results and experiments? So far there is no systematic experimental study of the critical adsorption and the near-critical solvation force as a function of bulk and surface fields in confined systems. Experimental studies of the critical adsorption in fluids concern primarily the universal behavior in the limit of strong adsorption $h_1 \rightarrow \infty$ and have been performed in the semi-infinite geometry, such as, for example, binary liquid mixtures adsorbed at a single solid substrate or more usually at a fluid interface [22]. The strong adsorption limit was also studied in a confined geometry. These experiments have been performed for pure fluids and employed adsorbents with a large surface area, such as finely divided (colloidal) graphite or a porous glass [23]. Colloidal particles or mesopores exert confining effects on the near-critical fluids and our results might be of relevance for such systems. In fluid experiments $h \sim \mu - \mu_c(T)$, where $\mu_c(T)$ is the critical chemical potential, and this is determined by the density of a fluid in the reservoir. Our findings imply that a slight change in the density of the reservoir can lead to pronounced deviation from the universal behavior, a rapid change in the adsorption, and the increase of the strength of the solvation force, which may lead to an agglomeration of the colloidal particles. Therefore the measurements near bulk criticality of a fluid requires

high precision, not only in the temperature. Moreover, our results indicate a qualitatively different behavior for $h_1 h > 0$ and $h_1 h < 0$. For fluids confined between adsorbing walls, it means a different behavior on the liquid and on the gas side of the coexistence line, even very close to μ_c . On a gas side the deviations from the behavior corresponding to the bulk phase coexistence $\mu = \mu_c$, is much stronger than on the liquid side. Thus, in experimental studies focusing on critical systems, $h=0$ ($\mu = \mu_c$), it is essential to choose $h \rightarrow 0$, such that $h_1 h > 0$.

Precise determination of the strength of the surface field h_1 for a particular fluid-adsorbent system, is difficult. Hence, there are only two experimental studies of the critical adsorption as a function of h_1 reported in the literature. Both concern binary liquid mixtures adsorbed at a *single* surface. In the pioneering work [24] the adsorbing solid surface has been chemically modified during the experiment thus changing with time its preference from one component to another. In the most recent work a homologous series of critical mixtures were adsorbed at the liquid vapor interface [25]. During the experiment, one of the components has been varied by increasing the chain length so that its surface energy progressively increases and the preference in the adsorption changes from the one component to the other. h_1 was related to the surface energy difference between two components. Both ways of changing the strength of the surface field could be used for studying the confined systems.

Quantitatively, our results are relevant for $d=2$ systems, such as monolayers adsorbed at a substrate, or fluids confined in slits very narrow in the third dimension. In this case h is related to the interactions with the substrate. In $d=3$ we expect qualitatively similar behavior, since the physical phenomena, such as the proximity of capillary condensation and the competition between length scales associated with h_1 , h , and L are not restricted to two dimensions. Finally, we note that choosing a fluid with desired adsorption properties, and/or changing a density of this fluid near bulk criticality, provide a mechanism for tuning the effective interactions between large colloidal particles immersed in this fluid.

ACKNOWLEDGMENT

This work was partially funded by KBN Grant Nos. 2P03B10616 and 3T09A07316.

-
- [1] J. N Israelachvili, *Intermolecular and Surface Forces*, 2nd ed. (Academic, London, 1991).
 - [2] For a general review of critical behavior at surfaces, see K. Binder, *Phase Transitions and Critical Phenomena*, edited by C. Domb and J. L. Lebowitz (Academic, London, 1983), Vol. 8, p. 1.
 - [3] H. W. Diehl, *Phase Transitions and Critical Phenomena*, edited by C. Domb and J. L. Lebowitz (Academic, London, 1986), Vol. 10, p. 75, and references therein.
 - [4] A. Maciołek, A. Ciach, and A. Drzewiński, Phys. Rev. E **60**, 2887 (1999).
 - [5] U. Ritschel and P. Czerner, Phys. Rev. Lett. **77**, 3645 (1996), and references therein.
 - [6] A. Maciołek, A. Ciach, and R. Evans, J. Chem. Phys. **108**, 9765 (1998).
 - [7] A. Maciołek, R. Evans, and N. B. Wilding, Phys. Rev. E **60**, 7105 (1999).
 - [8] A. Drzewiński, A. Maciołek, and A. Ciach, Phys. Rev. E **61**, 5009 (2000).
 - [9] A. Drzewiński, A. Maciołek, and R. Evans, Phys. Rev. Lett. **85**, 3079 (2000).
 - [10] S. R. White, Phys. Rev. Lett. **69**, 2863 (1992).

- [11] T. Nishino, J. Phys. Soc. Jpn. **64**, 3598 (1995).
- [12] A. Drzewiński, A. Ciach, and A. Maciołek, Eur. Phys. J. B **5**, 825 (1998).
- [13] *Lectures Notes in Physics*, edited by I. Peschel, X. Wang, M. Kaulke, and K. Hallberg (Springer-Verlag, Berlin, 1999), Vol. 528.
- [14] L. Onsager, Phys. Rev. **65**, 117 (1944).
- [15] M. N. Barber, *Phase Transitions and Critical Phenomena*, edited by C. Domb and J. L. Lebowitz (Academic, London, 1983), Vol. 8, p. 145.
- [16] E. Carlon, A. Drzewiński, and J. Rogiers, Phys. Rev. B **58**, 5070 (1998).
- [17] For Monte Carlo results see E. V. Albano, K. Binder, and W. Paul, J. Phys. A **30**, 3285 (1997), and references therein.
- [18] M. E. Fisher and H. Nakanishi, J. Chem. Phys. **75**, 5857 (1981); H. Nakanishi and M. E. Fisher, *ibid.* **78**, 3279 (1983).
- [19] R. Evans, U. Marini Bettolo Marconi, and P. Tarazona, J. Chem. Phys. **84**, 2376 (1986).
- [20] R. Z. Bariev, Theor. Math. Phys. **77**, 1090 (1988).
- [21] E. V. Albano, K. Binder, D. W. Heermann, and W. Paul, J. Chem. Phys. **91**, 3700 (1991).
- [22] (a) S. Dietrich, in *Phase Transition and Critical Phenomena*, edited by C. Domb and J. Lebowitz (Academic, London, 1988), Vol. 12, p. 1; (b) H. Dosch, in *Critical Phenomena at Surfaces and Interfaces*, edited by G. Höhler and E. A. Niekisch, Springer Tracts in Modern Physics Vol. 126 (Springer-Verlag, Berlin, 1992), p. 1, and references therein; (c) D. Beysens, in *Liquids at Interfaces*, edited by J. Charvolin, J. F. Joanny, and J. Zinn-Justin (North-Holland, Amsterdam, 1988); (d) G. Flöter and S. Dietrich, Z. Phys. B: Condens. Matter **97**, 213 (1995); (e) J. H. Carpenter *et al.*, Phys. Rev. E **59**, 5655 (1999); **61**, 532 (2000).
- [23] S. Blümel and G. H. Findenegg, Phys. Rev. Lett. **54**, 447 (1985); M. Thommes, G. H. Findenegg, and H. Lewandowski, Ber. Bunsenges. Phys. Chem. **98**, 477 (1994); M. Thommes, G. H. Findenegg, and M. Schoen, Langmuir **11**, 2137 (1995).
- [24] N. S. Desai, S. Peach, and C. Franck, Phys. Rev. E **52**, 4129 (1995).
- [25] J.-H. J. Cho and B. M. Law, Phys. Rev. Lett. **86**, 2070 (2001).